Circulation

JOURNAL OF THE AMERICAN HEART ASSOCIATION

American Heart Association®

Learn and Live℠

Absence of Thrombospondin-2 Causes Age-Related Dilated Cardiomyopathy

Melissa Swinnen, Davy Vanhoutte, Geert C. Van Almen, Nazha Hamdani, Mark W.M. Schellings, Jan D'hooge, Jolanda Van der Velden, Matthew S. Weaver, E. Helene Sage, Paul Bornstein, Fons K. Verheyen, Thierry VandenDriessche, Marinee K. Chuah, Dirk Westermann, Walter J. Paulus, Frans Van de Werf, Blanche Schroen, Peter Carmeliet, Yigal M. Pinto and Stephane Heymans

Circulation 2009, 120:1585-1597: originally published online October 5, 2009
doi: 10.1161/CIRCULATIONAHA.109.863266
Circulation is published by the American Heart Association. 7272 Greenville Avenue, Dallas, TX 72514
 Print ISSN: 0009-7322. Online ISSN: 1524-4539

Absence of Thrombospondin-2 Causes Age-Related Dilated Cardiomyopathy

Melissa Swinnen, MS*; Davy Vanhoutte, PhD*; Geert C. Van Almen, MS; Nazha Hamdani, PhD; Mark W.M. Schellings, PhD; Jan D'hooge, PhD; Jolanda Van der Velden, PhD; Matthew S. Weaver, PhD; E. Helene Sage, PhD; Paul Bornstein, MD; Fons K. Verheyen, PhD; Thierry VandenDriessche, PhD; Marinee K. Chuah, PhD; Dirk Westermann, MD; Walter J. Paulus, MD, PhD; Frans Van de Werf, MD, PhD; Blanche Schroen, PhD; Peter Carmeliet, MD, PhD; Yigal M. Pinto, MD, PhD; Stephane Heymans, MD, PhD

Background—The progressive shift from a young to an aged heart is characterized by alterations in the cardiac matrix. The present study investigated whether the matricellular protein thrombospondin-2 (TSP-2) may affect cardiac dimensions and function with physiological aging of the heart.

Methods and Results—TSP-2 knockout (KO) and wild-type mice were followed up to an age of 60 weeks. Survival rate, cardiac function, and morphology did not differ at a young age in TSP-2 KO compared with wild-type mice. However, >55% of the TSP-2 KO mice died between 24 and 60 weeks of age, whereas <10% of the wild-type mice died. In the absence of TSP-2, older mice displayed a severe dilated cardiomyopathy with impaired systolic function, increased cardiac dilatation, and fibrosis. Ultrastructural analysis revealed progressive myocyte stress and death, accompanied by an inflammatory response and replacement fibrosis, in aging TSP-2 KO animals, whereas capillary or coronary morphology or density was not affected. Importantly, adeno-associated virus-9 gene–mediated transfer of TSP-2 in 7-week-old TSP-2 KO mice normalized their survival and prevented dilated cardiomyopathy. In TSP-2 KO animals, age-related cardiomyopathy was accompanied by increased matrix metalloproteinase-2 and decreased tissue transglutaminase-2 activity, together with impaired collagen cross-linking. At the cardiomyocyte level, TSP-2 deficiency in vivo and its knockdown in vitro decreased the activation of the Akt survival pathway in cardiomyocytes.

Conclusion—TSP-2 expression in the heart protects against age-dependent dilated cardiomyopathy. **(*Circulation*. 2009; 120:1585-1597.)**

Key Words: aging ■ cardiomyopathy ■ heart failure ■ myocytes ■ remodeling

Whether aging of the heart and related functional changes should be regarded as a physiological or pathological process is a puzzling question. In the absence of other diseases such as hypertension and diabetes mellitus or detrimental environmental factors such as smoking, the heart is perfectly able to "survive" for a human lifespan. Hence, disease processes such as lamin A/C mutations that result in accelerated aging of the heart and dilated cardiomyopathy point toward essential protective mechanisms that are mandatory for normal physiological aging of the heart.[1,2]

Clinical Perspective on p 1597

The extracellular matrix is a crucial system that hinders functional and structural deterioration of the heart with aging. Matrix elements not only provide structural support, as collagen does, but also are implicated in maintaining cellular homeostasis and regulating intracellular signaling during normal cardiac physiology.[2] Thrombospondin-2 (TSP-2) belongs to a family of nonstructural matricellular proteins implicated in regulating cell-matrix interactions. Its expres-

Received March 13, 2009; accepted August 17, 2009.

From the Center for Heart Failure Research (M.S., G.C.V.A., M.W.M.S., B.S., S.H.) and Department of Molecular Cell Biology (F.K.V.), CARIM, Maastricht University, Maastricht, the Netherlands; Vesalius Research Center, K.U. Leuven and VIB, Leuven, Belgium (M.S., D.V., T.V., M.K.C., P.C.); Laboratory for Physiology, Institute for Cardiovascular Research, VU University Medical Center, Amsterdam, the Netherlands (N.H., J.V.d.V., W.J.P.); Department of Cardiovascular Diseases, K.U. Leuven, Leuven, Belgium (D.V., J.D., F.V.d.W.); Hope Heart Program, Benaroya Research Institute at Virginia Mason, Seattle, Wash (M.S.W., E.H.S.); Departments of Biochemistry and Medicine, Washington University, Seattle (P.B.); Department of Cardiology and Pneumology, Charité-Universitätsmedizin Berlin, Campus Benjamin Franklin, Berlin, Germany (D.W.); and Heart Failure Research Center, University of Amsterdam, Amsterdam, the Netherlands (Y.M.P.).

*The first 2 authors contributed equally to this work.

The online-only Data Supplement is available with this article at http://circ.ahajournals.org/cgi/content/full/CIRCULATIONAHA.109.863266/DC1.

Correspondence to Stephane Heymans, MD, PhD, Center for Heart Failure Research, CARIM, Department of Cardiology, Maastricht University Medical Center, PO BOX 5800, 6202 AZ Maastricht, the Netherlands. E-mail s.heymans@cardio.unimaas.nl

Circulation **is available at http://circ.ahajournals.org** **DOI: 10.1161/CIRCULATIONAHA.109.863266**

sion is low in the normal postnatal heart but reappears at high levels during cardiac pathology[3,4] and helps to preserve cardiac integrity during hypertension.[5] However, its function in normal physiological aging of the heart remains unknown. We therefore investigated whether TSP-2, by affecting survival pathways in cardiomyocytes, may provide necessary molecular support for the heart with aging and thus increase lifespan. We provide data showing that hearts lacking TSP-2 progress toward dilated cardiomyopathy with advanced age but have normal morphology and function at a young age. Importantly, postnatal adeno-associated viral vector (AAV9)–mediated transfer of TSP-2 in young TSP-2 knockout (KO) mice completely normalized their survival and prevented the development of cardiac failure. With aging, lack of TSP-2 resulted in decreased activation of the Src/Akt survival pathway, increased matrix metalloproteinase 2 (MMP-2) activity, and decreased collagen cross-linking, leading to progressive cardiomyocyte dropout and overall cardiac failure and dilatation.

Materials and Methods

See the online-only Data Supplement for additional details.

Transgenic Mice and Experimental Procedures

This study was approved by the Institutional Animal Research committees, and all experiments were performed according to official rules formulated under Dutch and Belgian law on the care and use of experimental animals. Eight- to 60-week-old TSP-2 KO mice and their wild-type (WT) littermates on a C57Bl6/129SvJ/EMS+Ter genetic background were used.[6] At a young age, male and female mice were divided into 3 age groups for further analysis: young mice, 8 to 12 weeks old (n=20 for TSP-2 WT mice, n=20 for TSP-2 KO mice); intermediate-age mice, 25 to 30 weeks old (n=20 for TSP-2 WT mice, n=20 for TSP-2 KO mice); and older mice, 50 to 60 weeks old (n=100 for TSP-2 WT mice, n=100 for TSP-2 KO mice). Consequently, only mortality rates within the third group were included in the survival curve.

Next, to rescue cardiac TSP-2 expression, AAV9 gene transfer of TSP-2 was performed in TSP-2 KO mice. Additional details on the construction and production of the AAV9–TSP-2 and AAV9–green fluorescent protein (GFP) vectors, with both TSP-2 and GFP driven under the cytomegalovirus promoter, are provided in the online-only Data Supplement. We injected 100 μL containing 1×10^{11} viral genomic copies of AAV9–TSP-2 or the control AAV9-GFP intravenously into the tail vein of adult (7-week-old) male (n=10 for AAV9–TSP-2, n=25 for AAV9-GFP) and female (n=19 for AAV9–TSP-2, n=10 for AAV9-GFP) TSP-2 KO mice and monitored them until 60 weeks of age. All analyses were performed following standard operating procedures and confirmed by independent observers blinded to genotype or treatment group.

Cardiac Function, Histopathological, and Molecular Analyses

After the study period, all mice were anesthetized, followed by transthoracic echocardiographic examination. Subsequently, hearts were taken out and prepared for further histological and molecular analysis, including immunohistochemical and electron microscopic analysis, determination of zymographic MMP and tissue transglutaminase (tTG) activity with aging, RNA isolation and real-time polymerase chain reaction, immunoblotting, integrin-linked kinase (ILK) activity and active transforming growth factor-β (TGF-β) assays, in vitro experimental approaches, force measurements in single permeabilized cardiomyocytes, and phosphorylation status of myofilament proteins. Experimental materials and methods are described more extensively in the online-only Data Supplement.

Statistical Analysis

All data are expressed as mean±SEM. Mann–Whitney *U* test, unpaired *t* test, or 2-way ANOVA was used as appropriate to assess statistical significance between groups. Survival curves were obtained by the Kaplan–Meier method and compared by the log-rank test. A 2-sided value of $P<0.05$ was considered statistically significant.

Results

TSP-2 KO Mice Develop Accelerated Aging-Induced Cardiomyopathy

To investigate the effect of TSP-2 on aging, a prospective study for mortality was conducted (Figure 1A). Whereas no significant mortality was noted until 20 weeks of age, the survival rate of TSP-2 KO mice progressively declined thereafter compared with WT mice (Figure 1A). By 60 weeks of age, 55% of the TSP-2 KO mice died (55 of 100), whereas 90% of the WT mice (90 of 100) remained alive ($P<0.01$). Interestingly, mortality was significantly higher in male (84%, 42 of 50) compared with female (26%, 13 of 50) TSP-2 KO mice ($P<0.01$; Figure 1A).

TSP-2 transcript and protein levels were significantly increased (3.4- and 3.6-fold, respectively) in older compared with young TSP-2 WT hearts (Table 1 and Figure 1B). Moreover, immunoblotting revealed that TSP-2 protein levels were more elevated in older female compared with older male WT hearts (Figure 1B). Immunohistochemical analysis confirmed that TSP-2 protein expression was low in young WT hearts (Figure 1C) but abundantly present and located primarily in the extracellular matrix surrounding the cardiomyocytes in both older female and male TSP-2 WT hearts (Figure 1C).

To investigate whether the absence of TSP-2 resulted in compensatory changes in expression of other TSPs before the onset of heart failure, transcript and/or protein levels of TSP-1, -3, and -4 were determined in the hearts of young and older TSP-2 KO and WT mice (Table 1). Compared with WT hearts, a clear trend toward increased TSP-4 transcript levels was observed in TSP-2 KO hearts ($P=0.08$ at young age, $P=0.07$ at older age; Table 1). However, no significant differences in TSP-1, -3, and -4 transcript levels were noted between WT and KO hearts at both young and older age (Table 1). Concordantly, TSP-1 and -3 immunoblotting did not reveal any significant differences between the TSP-2 WT and KO hearts (Table 1).

Further analysis of the aged hearts revealed that the increased mortality was due to progressive and severe dilated cardiomyopathy, with increasing cardiac fibrosis and dilatation with aging in TSP-2 KO mice (Figure 1D through 1K and Tables 2 and 3). In concordance, echocardiographic analysis showed depressed systolic function and increased cardiac dilatation in surviving TSP-2 KO compared with older WT mice (Table 2). Cardiac fibrosis, dysfunction, and dilatation were more pronounced in the older male compared with the older female TSP-2 KO hearts (Figure 1D through 1K and Tables 2 and 3). Increased cardiac failure in TSP-2 KO mice was further validated by an increased ratio of lung to body weight compared with WT mice at 60 weeks (Table 2). At young age, cardiac function and dimensions did not

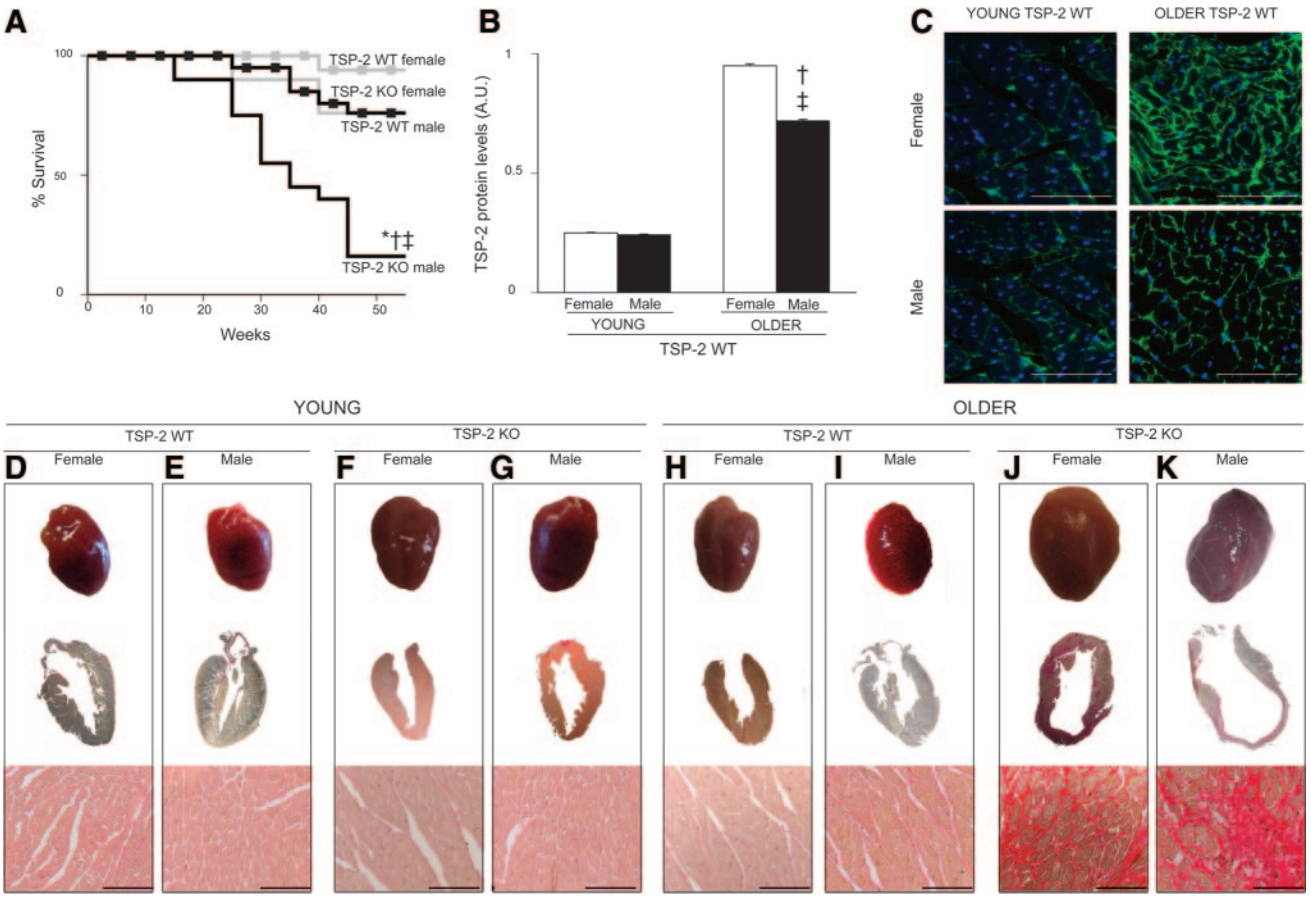

Figure 1. Age-induced dilated cardiomyopathy and increased mortality in the absence of TSP-2. A, Survival curves of TSP-2 KO and WT mice. B, Immunoblotting of TSP-2 in WT hearts. C, Increased TSP-2 immunofluorescent staining in older WT hearts. D through K, Macroscopic hearts (top) and Sirius red staining from young and older, male and female TSP-2 WT and KO mice. See also Figure I of the online-only Data Supplement. *$P<0.01$, TSP-2 KO mice vs TSP-2 WT mice within the same gender and age; †$P<0.01$, older TSP-2 mice vs younger TSP-2 mice within the same genotype; ‡$P<0.01$, TSP-2 female mice vs TSP-2 male mice with the same genotype within the same age group. Bars=100 μm (C through K).

differ in TSP-2 KO compared with age-matched WT animals (Table 2).

Structural Features of Accelerated Aging of the Heart in TSP-2 KO Mice

To study the underlying mechanisms of the age-related cardiomyopathy, the morphological features of cardiomyocytes, interstitial matrix, and vessels, including markers of apoptosis and cell stress, were examined within the surviving male and female TSP2 WT and KO hearts at young (8 to 12 weeks), intermediate (25 to 30 weeks), and older (50 to 60 weeks) age.

Histopathological analysis revealed a progressive decrease in cardiomyocyte density and increase in scar-forming fibrosis with advanced age in the male and female TSP-2 KO hearts but not in aged WT hearts (Figure 1D through 1K, Table 3, and Figure I of the online-only Data Supplement). No differences were seen at young age. Cardiomyocyte dropout was further indicated by a significantly reduced ratio of left ventricular weight to body weight in older TSP-2 KO mice, whereas this ratio did not differ between young WT and TSP-2 KO mice (Figure 1D through 1K and Table 3). Myocyte stress in older TSP-2 KO hearts was confirmed by desmin staining,[7] revealing a clear desmin disorganization (Figure 2A). Ubiquitin, a marker of cell stress, and p16, an indicator of aging,[8] were significantly increased in older TSP-2 KO hearts (Figure 2B and 2C and Table 3).

Electron microscopy substantiated cardiomyocyte stress and a disorganization of the extracellular matrix in older TSP-2 KO compared with WT hearts, whereas myocytes and matrix were normal in younger TSP-2 KO and WT hearts (Figure 2E and 2F). Cardiomyocytes of old TSP-2 KO hearts showed mitochondrial enlargement and lysis of myofilaments (Figure 2E and 2F).

Decreased cardiac mass was not due to significant changes in myocyte cross-sectional area of older TSP-2 KO hearts compared with age-matched WT hearts (Table 3). Myocyte death and fibrosis were not caused by differences in vascularity (Table 3).

AAV9–TSP-2 Treatment of TSP-2 KO Mice Prevents Accelerated Aging-Induced Cardiomyopathy

To determine whether the age-related cardiomyopathy in TSP-2 KO mice could be rescued by postnatal gene transfer of TSP-2, we treated young male and female TSP-2 KO mice

Table 1. Transcript and Protein Levels of TSPs, Oxidative Stress, and Inflammatory Markers

	Young		Older	
	WT (n=5)	KO (n=5)	WT (n=5)	KO (n=5)
TSPs				
Relative mRNA expression, AU				
TSP-1	1.2±0.37	1.9±0.53	1.1±0.35	1.5±0.43
TSP-2	1.0±0.10	<0.1	3.4±0.55†	<0.1*
TSP-3	1.1±0.23	2.2±0.35	1.3±0.49	1.7±0.27
TSP-4	1.1±0.28	5.5±2.1	1.1±0.35	5.8±2.7
Protein levels, AU				
TSP-1	0.52±0.03	0.62±0.05	0.55±0.10	0.60±0.13
TSP-2	0.23±0.01	<0.1*	0.82±0.05†	<0.1*
TSP-3	0.54±0.04	0.59±0.09	0.61±0.03	0.66±0.15
Oxidative stress				
Relative mRNA expression, AU				
CAT1	1.7±1.0	1.6±0.9	2.9±0.2†	2.1±0.1*†
SOD2	1.0±0.1	0.71±0.1	6.6±1.5†	6.5±1.2†
GXP1	1.0±0.01	0.99±0.7	1.0±0.5*	1.0±0.4
Inflammation				
Protein levels, pg/mL				
TGF-β	4.7±1.0	6.2±1.1	5.0±0.9	4.6±0.8
Relative mRNA expression, AU				
TGF-β	1.0±0.2	1.0±0.9	0.15±0.05†	0.2±0.02*†
IL-1 beta	<0.05	<0.05	1.0±0.5†	4.6±0.2*†
IL-6	<0.05	<0.05	1.0±0.2	3.8±0.4*†
IL-12	1.0±0.9	1.0±0.5	0.96±0.05†	8.7±0.9*†

AU indicates arbitrary units.
*$P<0.05$, TSP-2 WT vs TSP-2 KO mice within the same age group and gender.
†$P<0.05$, young vs older mice with the same genotype.

with AAV9–TSP-2 compared with control AAV9-GFP (Figure 3A through 3F). At 60 weeks of age, both immunoblotting and immunostaining revealed that AAV9-mediated transfer of TSP-2 resulted in significant and widespread cardiac TSP-2 protein expression, whereas TSP-2 staining was absent in the control AAV9-GFP–treated mice (Figure 3B through 3F).

Importantly, AAV9–TSP-2 blunted the mortality observed in the older control AAV9-GFP–treated TSP-2 KO mice (68%, 24 of 35: 3 of 10 females and 21 of 25 males; Figure 3A). AAV9–TSP-2 also prevented cardiomyocyte dropout, fibrosis, and cardiac dilatation and dysfunction, still present in the aged control-treated TSP-2 KO mice (Figure 3A through 3F and Table 4). Together, these data confirm that

Table 2. In Vivo Cardiac Function in TSP-2 WT and KO Mice

	Young			Intermediate				Older				
	WT Female (n=6)	WT Male (n=6)	KO Female (n=7)	KO Male (n=7)	WT Female (n=6)	WT Male (n=6)	KO Female (n=6)	KO Male (n=6)	WT Female (n=5)	WT Male (n=5)	KO Female (n=10)	KO Male (n=4)
LV/BW, mg/g	3.7±0.1	3.9±0.3	3.8±0.1	4.0±0.2	3.9±0.1	3.8±0.2	3.8±0.2	3.9±0.1	4.1±0.1	4.2±0.3	3.4±0.3*†	3.1±0.5*†‡
Lung/BW ratio, mg/g	3.8±0.2	3.9±0.1	4.2±0.2	4.3±0.1	4.0±0.1	4.1±0.1	4.1±0.1	4.2±0.1	6.4±0.4	6.6±0.4	10.5±1.2*†	12±1.6*†‡
Diastolic PW, mm	0.90±0.02	0.90±0.03	0.93±0.05	0.90±0.05	0.92±0.05	0.92±0.02	0.90±0.03	0.89±0.05	0.83±0.05	0.87±0.05	0.80±0.05	0.76±0.07
Diastolic SW, mm	0.89±0.05	0.87±0.05	0.85±0.02	0.87±0.02	0.90±0.05	0.90±0.05	0.93±0.02	0.92±0.02	0.95±0.05	0.8±0.05	0.82±0.02	0.86±0.06
LVEDD, mm	2.9±0.1	3.0±0.1	2.6±0.1	3.0±0.1	2.9±0.1	3.0±0.1	3.0±0.1	3.2±0.1	2.6±0.05	2.9±0.1	3.2±0.1*	3.6±0.1*†‡§
LVESD, mm	1.8±0.1	1.8±0.1	1.8±0.1	1.9±0.1	1.9±0.1	1.9±0.1	1.9±0.1	2.0±0.1	1.9±0.1	1.9±0.2	1.9±0.15	2.0±0.2
FS, %	38±0.8	36±1.6	36±1.6	37±2	37±1.0	37±1.0	36±1.1	32±1.7†	36±0.12	35±1.0	34±2.6	28±2.2*†‡§
Heart rate, bpm	550±6	550±10	560±9	560±10	550±5	555±6	555±7	550±8	560±12	560±10	570±12	557±10

LV indicates left ventricular; BW, body weight; Diastolic PW, left ventricular posterior wall in end diastole; Diastolic SW, septal wall thickness; LVEDD, left ventricular end-diastolic dimension; LVESD, left ventricular end-systolic dimension; and FS, fractional shortening.
*$P<0.05$, TSP-2 WT mice vs TSP-2 KO mice within the same age group and gender.
†$P<0.05$, older or intermediate-age TSP-2 mice vs young TSP-2 mice with the same genotype and gender.
‡$P<0.05$, older TSP-2 mice vs intermediate-age TSP-2 mice with the same genotype and gender.
§$P<0.05$, TSP-2 female mice vs TSP-2 male mice with the same genotype within the same age group.

Table 3. Morphological Characteristics of TSP-2 WT and KO Mice

	Young				Intermediate				Older			
	WT Female (n=6)	WT Male (n=6)	KO Female (n=7)	KO Male (n=7)	WT Female (n=6)	WT Male (n=6)	KO Female (n=6)	KO Male (n=6)	WT Female (n=5)	WT Male (n=5)	KO Female (n=10)	KO Male (n=4)
Collagen deposition, %	1.8±0.9	1.9±0.9	2.0±1.0	2.2±1.0	3.2±1.2	4.9±1.0†	8.2±1.2‡	20.4±3.1†,‡,§	2.9±0.5	5.4±3.5	10.3±4.2*†‡	26.3±3.7*†‡§
Ratio of orange-red thick to yellow-green thin fibers	9.5±1.5	8.9±1.3	5.7±0.7	6.0±0.9	9.2±1.5	9.4±1.1	4.8±0.5	6.1±0.7	8.9±1.4	9.9±1.6	2.9±0.8*‡	5.9±1.2*§
Desmin, score	5.9±0.5	9.6±0.6	7.2±0.7	9.9±0.8	4.0±1.0	7.6±1.1	9.2±1.8	16±2.0†§	12.3±1.3‡	20.4±1.8‡§	19.8±2.0*†‡	30±2.9*†§
Cardiomyocyte area, mm^2	230±2.1	230±4.1	280±10	240±14	250±2.0	290±6.2	290±10	320±10	347±15	345±20‡	352±20†‡	351±25†‡
Cardiomyocyte density, n/mm^2	2500±285	2320±95	2820±235	2430±75	2470±575	2300±65	2400±320	1850±300†§	2640±190	2600±200	1670±160*†‡	1290±220*†‡
Coronary density, n/mm^2	42±2.2	47±1.8	47±1.7	46±3.3	42±1.9	47±2.3	42±1.5	46±2.1	41±1.9	41±2.1	46±2.5	42±1.9
Capillary density, n/mm^2	5680±580	4220±350	5510±450	4170±420	5120±470	4150±260	5090±320	4099±280	4100±360	4200±430	4320±320	4020±290
Ubiqutin, %	2.7±0.07	2.9±0.05	2.9±0.07	3.3±0.05	2.9±0.06	3.0±0.07	3.1±0.06	3.6±0.04	3.8±0.08	3.6±0.05	6.7±1.0*,†,‡	18.6±2.5*†‡§
p16, %	<0.1	<0.1	<0.1	<0.1	<0.1	<0.1	2.1±1.2†	3.1±1.0†	5.5±1.0	6.2±1.4	9.3±1.9*†‡	14±2.1*†‡§
CD45, n/mm^2	40±8.0	42±10	41±6.0	39±4.0	42±9.0	35±11	98.7±11†	180±10†§	46±13	39±8	114±33*	226±13*§

*$P<0.05$, TSP-2 WT mice vs TSP-2 KO mice within the same age group and gender.
†$P<0.05$, older or intermediate-age TSP-2 mice vs young TSP-2 mice with the same genotype and gender.
‡$P<0.05$, older TSP-2 mice vs intermediate-age TSP-2 mice with the same genotype and gender.
§$P<0.05$, TSP-2 female mice vs TSP-2 male mice with the same genotype within the same age group.

postnatal TSP-2 expression is essential for maintaining myocardial architecture and function with age.

Increased Inflammation in Older TSP-2 KO Hearts

Next, we investigated whether a prolonged low-grade inflammation in response to aging-associated free radical generation could underlie the age-related cardiomyopathy observed in TSP-2-KO mice.[9] Cardiac aging and progressive myocyte stress in the absence of TSP-2 were accompanied by increased inflammation. The number of CD45-positive inflammatory cells increased progressively with age, reaching significance in TSP-2 KO compared with WT hearts at older age (Figure 2D and Table 3), but no significant differences were noticed at young age (Figure 2D and Table 3). Inflammation was more pronounced in older male compared with female TSP-2 KO mice (Figure 2D and Table 3). In concordance, cardiac transcript levels of TGF-β1 and interleukin (IL) -1β, IL-6, and IL-12 significantly increased with age and in older TSP-2 KO compared with WT hearts (Table 1). The activation of TGF-β1 did not differ (Table 1). In addition, transcript levels of enzymes influencing the oxidation status of the heart, including superoxide dismutase-2 and glutathione peroxidase-1, did not significantly differ between TSP-2 WT and KO hearts (Table 1), whereas catalase-1[10] was significantly higher in older WT compared with KO hearts (Table 1). In conclusion, age-related cardiomyopathy in the absence of TSP-2 is due to progressive cardiomyocyte stress and dropout, accompanied by increased inflammation and scar-forming reparative fibrosis.

Higher MMP-2 and Lower tTG-2 Activity in TSP-2 KO Mice

Previous studies have shown that a lack of TSP-2 results in an increase in MMP-2 activity, which in turn inactivates tTG-2. The latter enzyme is involved in collagen cross-linking and may protect against cardiac dilatation and dysfunction.[11,12] To investigate whether the increased cardiac dilatation in the absence of TSP-2 may relate to increased MMP-2 and consequently decreased tTG activity, their activity levels were measured in young and older TSP-2 KO and WT hearts.

Whereas no significant differences were noted in TSP-2 KO hearts, MMP-2 zymographic activity decreased significantly in TSP-2 WT hearts with progressing age (Figure 4A). MMP-2 activity levels were significantly lower in young KO compared with WT hearts but significantly higher in older KO compared with older WT hearts. MMP-9 zymographic activity did not differ significantly in TSP-2 KO compared with WT hearts at both young or old age (Figure 4B).

Decreased MMP-2 activity with progressing age in TSP-2 WT hearts was paralleled by increased tTG activity (Figure 4C). Concordantly, increased MMP-2 activity in older TSP-2 KO compared with older WT hearts was paralleled by reduced activity of tTG-2 and a decrease in ϵ-lysyl γ-glutaminyl cross-links (Figure 4D and 4E). A significant decrease in tTG-2 activity in TSP-2 KO compared with WT hearts was also observed at younger age (Figure 4A and 4C).

Sirius red–polarization microscopy revealed mainly well-aligned, thick, and tightly packed orange-red collagen fibers in young and older WT hearts. Loosely assembled yellow-green collagen fibers predominated the older TSP-2 KO hearts (Figure 4F and 4G and Table 3). Thus, increased MMP-2, decreased tTG-2 activity, and impaired collagen maturation in the absence of TSP-2 contributed to increased cardiac dilatation with aging.

Loss of TSP-2 Results in Impaired Activation of Akt In Vivo and In Vitro

The Akt pathway is centrally involved in promoting myocyte survival, and its activation protects against cardiac injury, fibrosis, and failure.[13,14] TSP-2 contains 2 conserved domains that are able to activate the Akt pathway, namely the

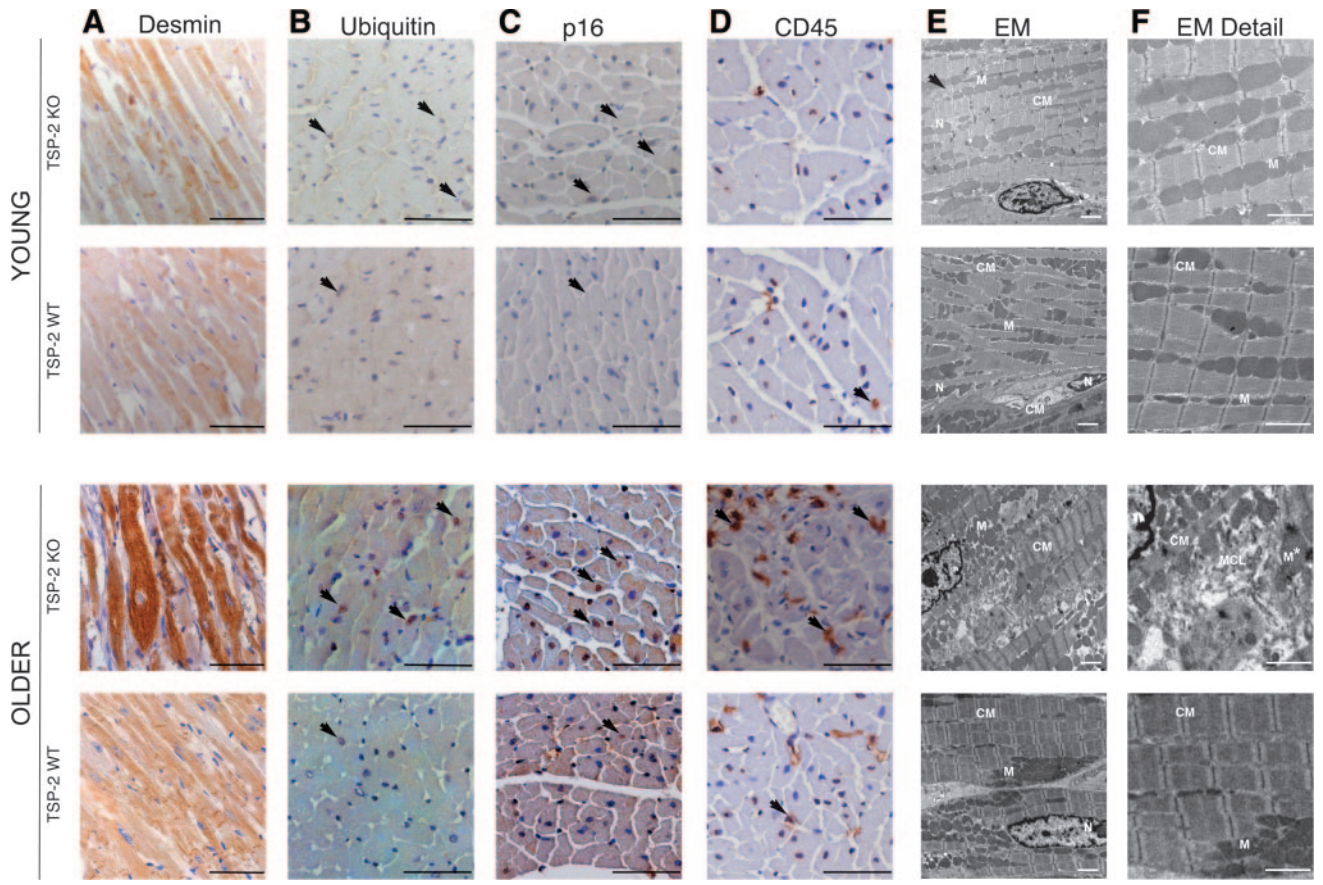

Figure 2. Structural features of accelerated aging of the hearts in TSP-2 KO mice. Histological and ultrastructural analyses of young and older male TSP-2 KO and WT hearts. Desmin (A) and ubiquitin (B), 2 markers of cell stress; p16, an indicator of aging (C); and infiltrating CD45-positive leukocytes (D) were increased in older TSP-2 KO hearts but did not differ at younger age. E and F, Electron microscopic analysis revealed increased myocytolytic damage and mitochondrial dilatation in older TSP-2 KO compared with WT hearts. Bars=50 μm (A through D), 2 μm (E), and 1 μm (F). N indicates nucleus; M, mitochondria; M*, dilated mitochondria; CM, cardiomyocyte; and MCL, myocytolytic damage.

CD47-binding site within its C-terminal domain and the N-terminal β1-integrin recognition site that is proximal to the CD36-binding domain.[15] Therefore, we investigated whether these interactions might contribute to the cardiomyocyte survival pathway.

First, significantly reduced activation of Src and Akt was demonstrated in TSP-2 KO compared with WT hearts (Figure 5A and 5B). Immunoblotting for ILK and in vitro kinase activity assays were performed to determine the relative level and activity of ILK in WT and TSP-2 KO hearts. However no differences in ILK activity could be detected in the hearts of TSP-2 WT and KO mice (Figure II of the online-only Data Supplement). Next, an interaction of TSP-2 with the Src/Akt pathway was confirmed in cardiac myocytes in vitro. The use of a lentiviral short-hairpin RNA produced an 80% knockdown of TSP-2 and resulted in significantly reduced phosphorylation of Src and Akt (Figure 5C through 5G), whereas a control, unrelated short-hairpin RNA lentiviral vector did not alter their phosphorylation status.

Finally, monoclonal blocking antibodies against either the CD47- (α-TSP^{CD47}) or the CD36- (α-TSP^{CD36}) binding sites of TSP were administered to neonatal rat cardiomyocytes in vitro (Figure 6A through 6C). Blocking of the TSP/CD47 interaction resulted in reduced phosphorylation of Src and Akt (Figure 6E through 6G) and caused obvious myocyte stress compared with control treatment. Here, myocyte stress was indicated by changes in the cytoskeletal organization as revealed by altered phalloidin staining, a significantly decreased cardiomyocyte density, and increased protein expression of activated caspase-3 (Figure 6A through 6D and 6H). Blocking of the CD36-binding site of TSP, however, did not significantly alter Src or Akt phosphorylation, nor did it change cardiomyocyte appearance or expression of activated caspase-3 (Figure 6A through 6H).

Absence of TSP-2 Affects Cardiomyocyte Function With Aging

To investigate the effect of age-related cardiomyopathy on the function of surviving cardiomyocytes, active and passive forces and Ca^{2+} sensitivity were determined through the use of individual permeabilized cardiomyocytes isolated from young and older TSP-2 KO and WT left ventricles. Passive and active forces and Ca^{2+} sensitivity did not differ in young TSP-2 KO compared with WT myocytes (n=10 cardiomyocytes from 5 hearts per group; P=NS; Figure 7A and 7B). Forces increased with advanced age in both TSP-2 KO and WT cardiomyocytes, but active forces did not differ between

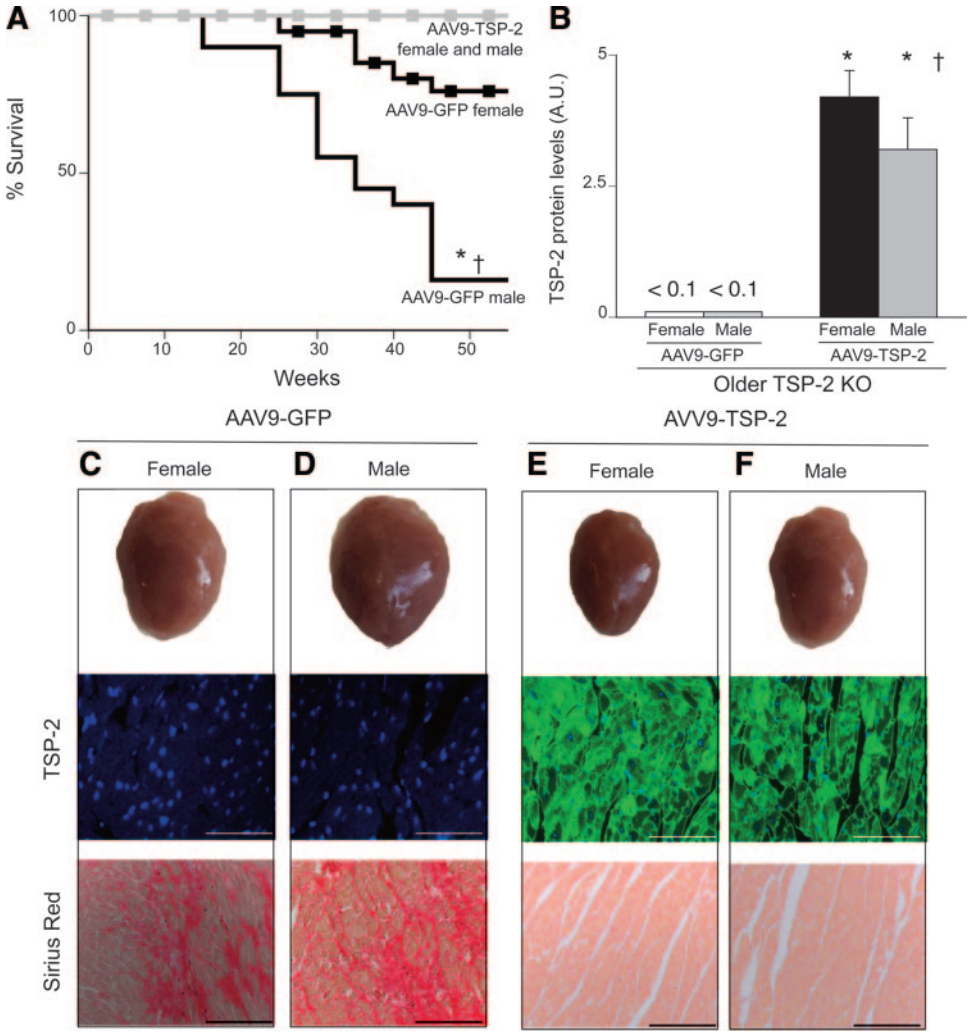

Figure 3. AAV9–TSP-2 treatment of TSP-2 KO mice prevents accelerated aging-induced cardiomyopathy. A, Survival curve of male and female AAV9-GFP– and AAV9–TSP-2–treated TSP-2 KO mice. B through F, At 60 weeks of age, both TSP-2 immunoblotting (B) and immunofluorescent staining (C through F, middle, green) confirmed a significant and widespread cardiac TSP-2 protein expression in AAV9–TSP-2– (B, E, and F) vs AAV9-GFP–treated TSP-2 KO mice (B through D; for B, n=5 per group). C through F, Top, Blunted cardiac dilatation in AAV9-GFP– (C and D) vs AAV9–TSP-2–treated TSP-2 KO mice (E and F). Bottom, Sirius red staining revealing blunted cardiac fibrosis in AAV9–TSP-2–treated TSP-2 KO mice. *$P<0.05$, AAV9-GFP treated vs AAV9–TSP-2–treated TSP-2 KO mice of the same gender; †$P<0.05$, TSP-2 female mice vs TSP-2 male mice with the same AAV9 treatment. Bars=100 μm (C through F).

TSP-2 KO and WT cardiomyocytes (Figure 7B). Passive forces were significantly higher in older TSP-2 KO compared with WT cardiomyocytes, indicating increased cardiomyocyte stiffness. Normalized force–P_{CA} curves showed similar myofilament Ca^{2+} sensitivity at young and older ages in TSP-2 WT and KO mice (data not shown). Impaired diastolic function of isolated cardiomyocytes was not due to an alteration in myofilament phosphorylation because treatment with the catalytic subunit protein kinase-A (PKA) provided similar effects in TSP-2 KO and WT cardiomyocytes (Figure 7C). PKA treatment resulted in nonsignificant reduced passive forces in young TSP-2 KO mice (passive force before PKA: WT, 1.4±0.2; KO, 2.3±0.5: passive force after PKA: WT, 1.1±0.1; KO, 1.8±0.4). Similarly, passive forces in the older mice did not change significantly. Phosphorylation levels of myosin binding protein c, myosin light chain 2, and troponin-T and -I did not significantly differ in TSP-2 KO compared with WT hearts at both young and older ages (Figure 7D).

Discussion

With advanced medical assistance and better control of cardiovascular risk factors, the general population is getting older, and many people may live to be >90 years of age without experiencing cardiac dysfunction. Still, little is known about the physiological survival mechanisms that help to "adapt" the heart and prevent myocyte death, fibrosis, and dysfunction in response to the cumulative hemodynamic stress related to aging. An understanding of these processes may lead to new therapeutic approaches that promote the longevity of the heart, even in the absence of hypertension, diabetes mellitus, smoking, or coronary disease.

We provide evidence that cardiac expression of the matricellular protein TSP-2 protects against aging-related functional decline of the heart. Loss of TSP-2 resulted in progressive cardiomyocyte death, accompanied by inflammation and reparative scar-forming fibrosis, all of which contributed to the development of progressive cardiac dilatation and dys-

Table 4. AAV9-Mediated Rescue of TSP-2 KO Mice

	AAV9-GFP		AAV9–TSP-2	
	KO Female (n=7)	KO Male (n=4)	KO Female (n=19)	KO Male (n=10)
Functional measurements				
LV/BW, mg/g	3.6±0.1	2.9±0.2	3.8±0.1	3.9±0.1*
Lung/BW ratio, mg/g	9.5±1.3	10.9±1.1	4.1±0.2*	4.1±0.1*
Diastolic PW, mm	0.81±0.02	0.77±0.05	0.96±0.01*	0.98±0.01*
Diastolic SW, mm	0.85±0.04	0.85±0.06	0.94±0.01*	0.94±0.01*
LVEDD, mm	3.1±0.2	3.5±0.2†	2.7±0.1*	2.7±0.1*
LVESD, mm	1.90±0.2	1.99±0.3	1.70±0.2*	1.70±0.2*
FS, %	33±1.2	29±0.9†	38±0.2*	37±0.7*
Heart rate, bpm	555±5.0	560±2.0	550±5.0	555±7.0
Histopathology				
Collagen deposition, %	9.5±0.5	24.3±0.3†	1.2±0.2*	1.4±0.1*
Cardiomyocyte density, n/mm^2	1630±170	1330±255†	2620±185*	2560±190*

Abbreviations as in Table 2.
*$P<0.05$, AAV9-GFP–treated vs AAV9–TSP-2–treated TSP-2 KO mice of the same gender.
†$P<0.05$, TSP-2 female mice vs TSP-2 male mice with the same AAV9 treatment.

function. Importantly, postnatal AAV9-mediated transfer of TSP-2 in young TSP-2 KO mice completely rescued the progressive structural and functional declines with aging.

In view of its matrix-cell–regulating properties, a protective role for TSP-2 against age-related heart disease may be mediated by regulating outward-inward cell signaling and function, thereby affecting cardiac remodeling. First, TSP-2 seems to protect against age-related myocyte death, at least in part, by promoting the Akt survival pathway in cardiomyocytes.[15] The absence of TSP-2 in vivo or its knockdown in

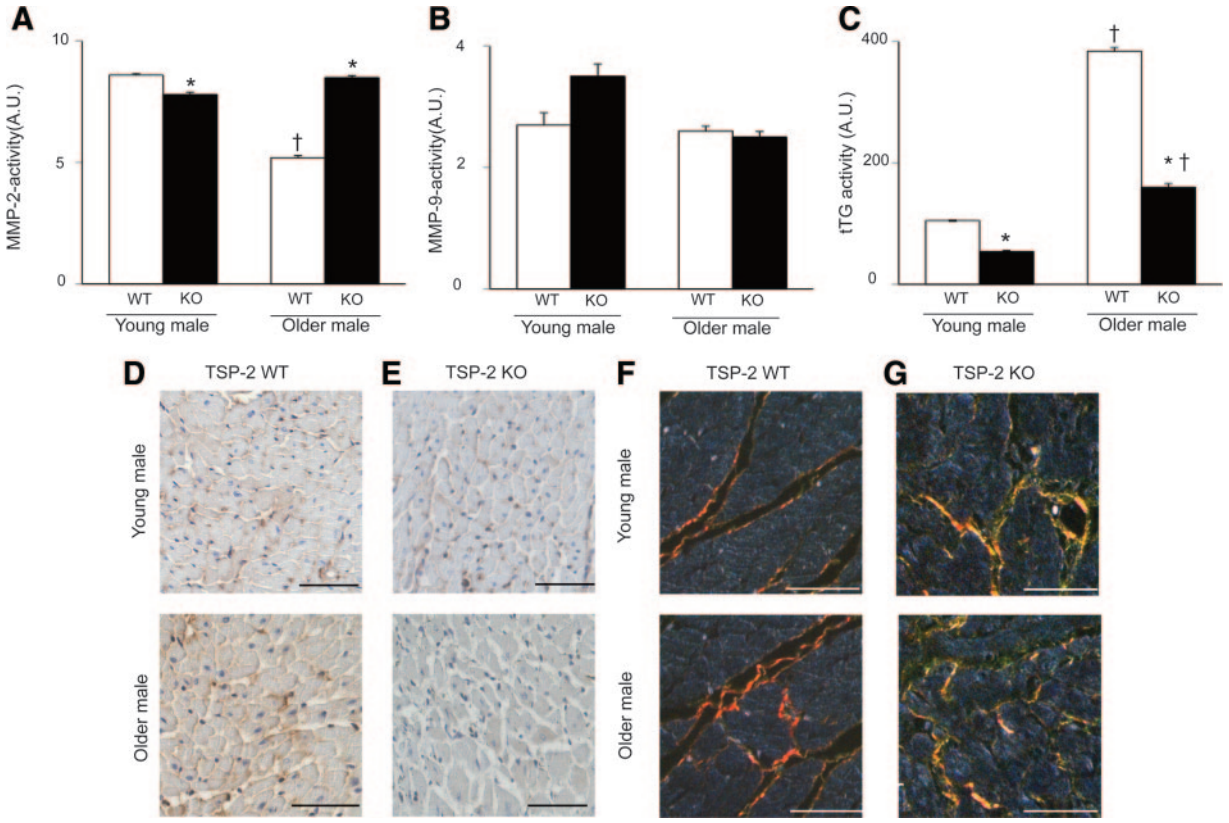

Figure 4. Higher MMP-2- and lower tTG-2 activity in TSP-2-KO mice. A, Significantly increased MMP-2 zymographic activity in older TSP-2 KO hearts. B, No significant differences in MMP-9 activity in TSP-2 WT vs KO mice. C, Significantly decreased levels of tTG-activity in TSP-2 KO aged hearts (n=7 per group). D and E, Decreased ϵ-lysyl-γ-glutaminyl crosslinking staining in older TSP-2 KO hearts (E and D, respectively; bottom). F and G, Sirius red–polarization microscopy revealing more loosely assembled (yellow-green) collagen fibers predominating in older TSP-2 KO hearts. *$P<0.05$, TSP-2 WT mice vs TSP-2 KO mice but within the same age group; †$P<0.05$, young TSP-2 mice vs older TSP-2 mice with the same genotype.

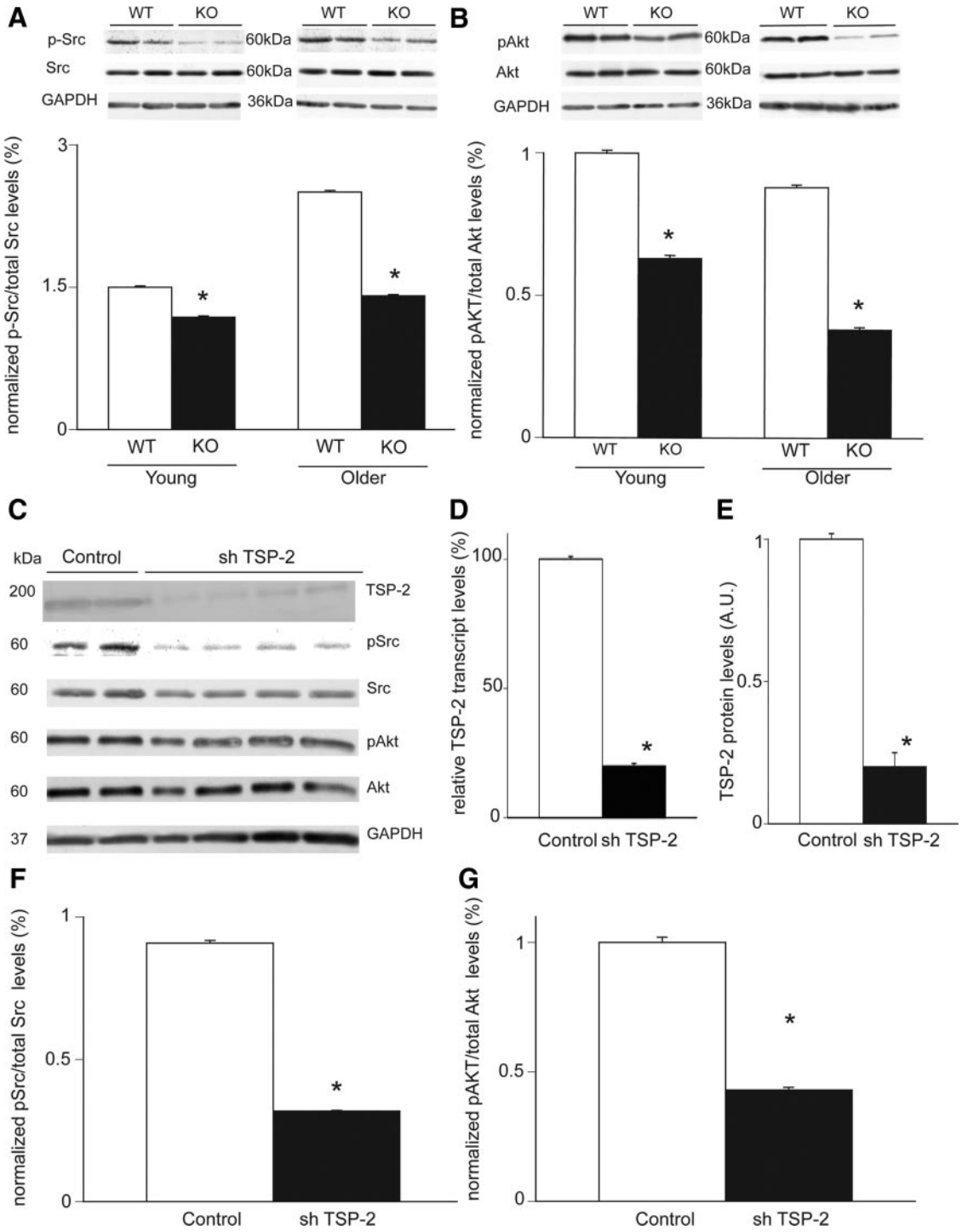

Figure 5. Loss of TSP-2 results in impaired Src/Akt-dependent cardiomyocyte survival in vivo and in vitro. A, B, Src protein levels and ratio of phosphorylated Akt to total Akt were significantly decreased in TSP-2 KO vs age-matched WT littermates (n=7 per group). C through G, In vitro experiments showing that knockdown for TSP-2 results in a significant reduction in Src and Akt phosphorylation in neonatal rat cardiomyocytes. All protein levels were normalized for GAPDH.

vitro resulted in reduced activation of Src and Akt, which are both involved in promoting myocyte survival.[13] Moreover, our data indicate that the conserved C-terminal CD47 binding of TSP-2 is implicated in activating the Src/Akt survival pathway in cardiomyocytes. A blocking antibody against the CD47-binding domain (α-TSP^{CD47}), but not against the CD36-binding domain (α-TSP^{CD36}), significantly reduced activation of Src/Akt and increased myocyte stress and apoptosis in vitro. To exclude that other upstream regulators are responsible for activating the effector protein Akt, the interaction with ILK was investigated in vivo. ILK functions downstream and independently of phosphatidylinositol 3-kinase to phosphorylate Akt. Immunoblotting for ILK, together with ILK activity measurements, did not show differences in KO and WT hearts. Together, our data indicate that the effect of TSP-2 on Akt phosphorylation is Src dependent. Previous

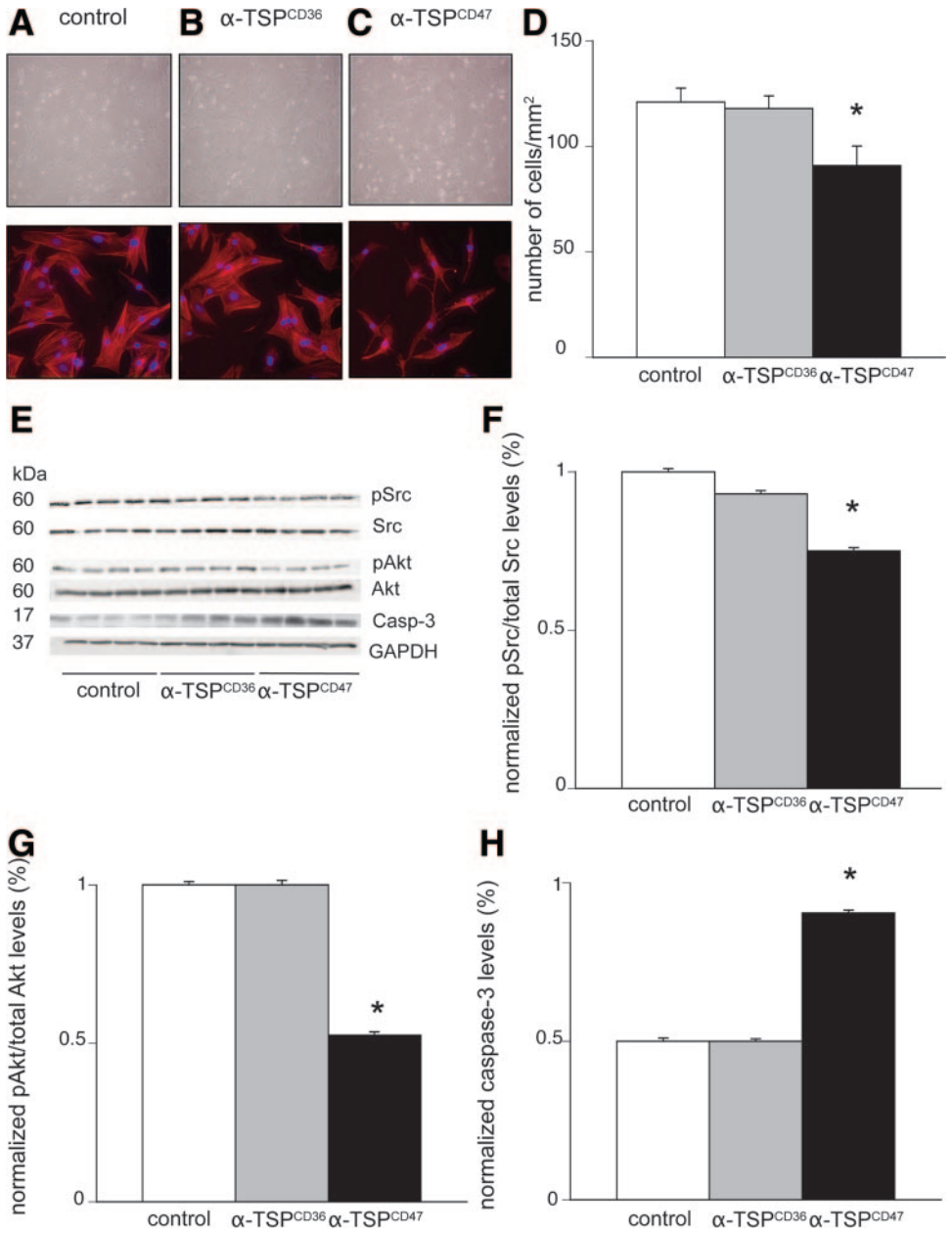

Figure 6. CD47 is involved in cardiac survival. Cell culture of neonatal rat cardiomyocytes treated with an α-TSP^{CD47}–blocking antibody (C) resulted in cytoskeletal impairment and a significantly decreased number of neonatal rat cardiomyocytes at 48 hours vs α-TSP^{CD36} (B) or the control group (untreated; A) (E through H). Decreased Src and Akt phosphorylation and increased active cleaved caspase-3 in α-TSP^{CD47}–treated neonatal rat cardiomyocytes (F through H; n=6 per treatment). *$P<0.05$.

reports have shown that the Akt pathway is regulated through several receptor and receptor-independent pathways (ie, mechanical stretch).[16,17] Concordantly, we cannot exclude that TSP-2 might also regulate myocyte survival by influencing other survival pathways, including ERK1-2 and p38-mitogen-activated protein kinases,[18] focal adhesion kinases,[19] or STAT3 signaling pathways.[20]

A protective role for TSP-2–mediated Akt activation in physiological aging, however, fits with a crucial role for Akt1 and Akt2 in physiological growth of cardiomyocytes during exercise; Akt1- or Akt2-deficient mice are not able to develop physiological hypertrophy during exercise but develop heart failure in response to pressure overload.[13,21] Moreover, the implication of outside-inside signaling and, more specifically, Akt activation in promoting (cardio)myocyte survival has also been demonstrated for other matricellular proteins. Periostin-[22] and CCN-1– (Cyr-61)[23] deficient mice have impaired myocyte survival resulting from reduced activation of the Akt survival pathway.

Beside its role in outside-inside signaling, TSP-2 also regulates extracellular matrix remodeling. It forms a complex with pro–MMP-2 and tissue inhibitor of metalloproteinase-2, which is then internalized by the low-density lipoprotein–related scavenger receptor LRP1 and thereby downregulates total MMP-2 activity.[24] MMP-2 in turn decreases total tTG activity[11] and may diminish the binding of TSP to CD47,

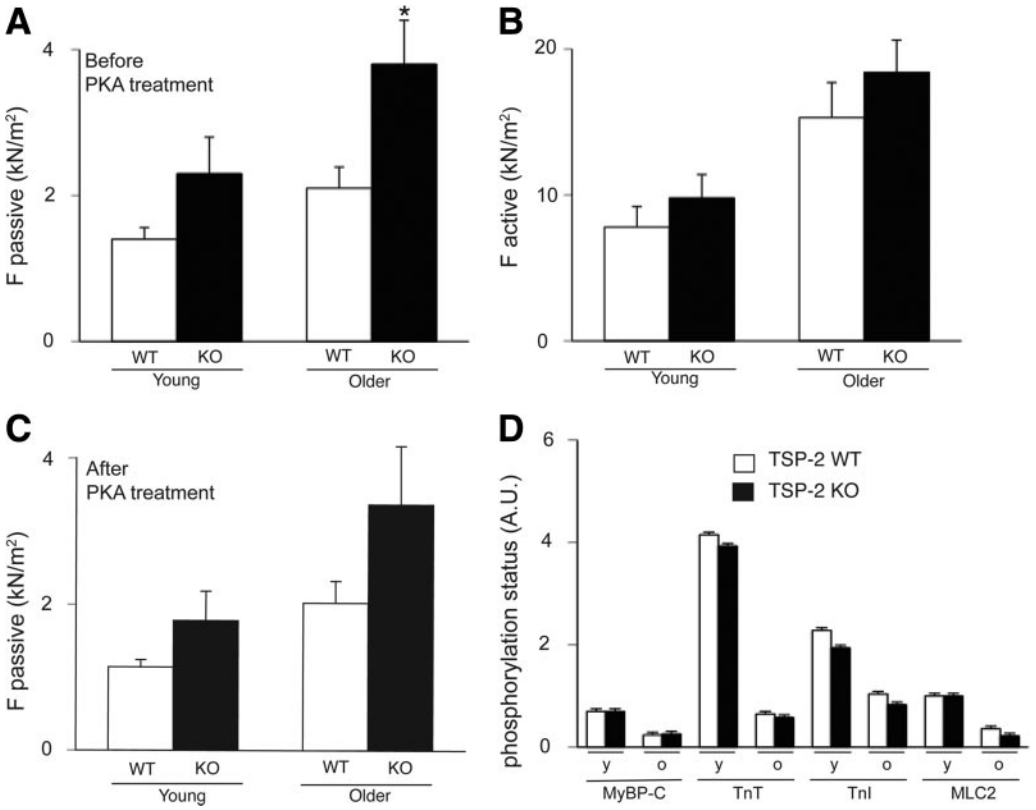

Figure 7. The absence of TSP-2 affects diastolic function of individual isolated cardiomyocytes. Passive forces (A) are significantly increased but active forces (B) are similar in TSP-2 KO vs WT myocytes. C, Exogenous PKA treatment did not change the differences in passive forces. D, Phosphorylation status of myosin-binding protein C (MyBP-C), troponin T (TnT), troponin I (TnI), and myosin light chain-2 (MLC-2) revealed no significant differences between TSP-2 WT and KO mice at young (y) and old (o) age (n=10 cardiomyocytes per genotype per age-group). *$P<0.05$, TSP-2 WT mice vs TSP-2 KO mice within the same age group.

thereby decreasing its downstream activity.[25] Aging in mice lacking TSP-2 results in increased MMP-2 activity, decreased tTG activity, and reduced collagen cross-linking, all contributing to increased cardiac dilatation and dysfunction.[2] In concordance, Agah et al[26] previously reported increased dermal TSP-2 expression and decreased clearance of MMP-2 from the pericellular environment as a function of age in TSP-2 WT mice.

TSP-2 was also shown to regulate angiogenesis and inflammation.[9,26,27] Here, we show that myocyte death and fibrosis with progressing age were not caused by differences in vascularity. However, inflammation was increased in the absence of TSP-2 in the older, but not in the younger, hearts. Both progressive cardiomyocyte death and the loss of the CD47-mediated antiinflammatory effect of TSP-2[9] might have contributed to this enhanced inflammatory influx. Whether the increased inflammatory response in aged TSP-2 KO mice acts mainly to remove the necrotic cardiomyocytes or whether the increased inflammation represents a primary contributing factor that aggravates cardiomyocyte injury, fibrosis, and age-related cardiomyopathy remains to be resolved.

The morphological and functional features of this age-related cardiomyopathy and mortality occurred mainly in male KO mice. Several previous studies have shown that female mice display a lower mortality and less severe cardiac pathology compared with their male counterparts.[28] Factors such as hormonal status, higher blood pressure, and increased physical activity may predispose male KO mice to severe myocardial damage, dilatation, and dysfunction and mortality compared with female mice with increasing age.[28–30]

Intriguingly, AAV9-mediated expression of TSP-2 in 7-week-old TSP-2 KO mice rescued this lethal phenotype, confirming that postnatal expression of TSP-2 is crucial for the normal physiological aging of the heart. These results also make it less probable that prenatal or early postnatal morphological changes in the heart of TSP-2 KO mice could underlie this progressive phenotype. Because of its cardiotrophic properties, AAV9-mediated gene transfer rescues a severe cardiac phenotype. AAV9-mediated gene transfer deserves to be further explored as a novel therapeutic tool for the clinical application of gene therapy in human cardiac diseases.[31]

To study whether aging of cardiomyocytes in the absence of TSP-2 may affect their function per se, isometric force measurements were performed in isolated, permeabilized cardiomyocytes. Active forces did not differ in aged TSP-2 KO compared with WT cardiomyocytes, whereas passive forces indicative of diastolic dysfunction were increased in the surviving TSP-2 KO cardiomyocytes. These alterations were independent of exogenous PKA activity, excluding myofilament phosphorylation as the underlying cause of cardiac dysfunction of isolated cardiomyocytes. Together, these data indicate that the surviving individual cardiomyocytes in the aged TSP-2 KO heart are characterized by

increased stiffness, whereas active forces are not affected. Thus, progressive myocyte death, but not reduced contractility of individual cardiomyocytes, is responsible for the progressive cardiac dysfunction in the absence of TSP-2.

Our present study reveals a novel and pivotal role for TSP-2 in the protection against age-related cardiomyopathy. Decreased activation of the Src/Akt survival pathway in the absence of TSP-2, together with increased inflammation, MMP-2 activity, and decreased collagen cross-linking, all contributed to impaired cardiomyocyte survival and increased cardiac dilatation and dysfunction with advanced age.

Conclusion

TSP-2 seems to represent a novel and crucial survival mechanism that protects against senescence of the heart.

Acknowledgments

We thank Rick van Leeuwen, Wouter Verhesen, Kevin Custers, and Hans Duimel for their technical support.

Sources of Funding

This study was supported by the Marie Curie Excellence Program to Dr Heymans, M. Swinnen, and Dr Pinto; a research grant from the Research Fund K.U. Leuven (PDMK/08/175) to Dr Vanhoutte; long-term structural funding–Methusalem funding by the Flemish government to Dr Carmeliet; a grant for SFB-TR 19 (project A2) to Dr Westermann from the Deutsche Forschungsgemeinschaft; a research grant from the Research Foundation Flanders (G.0601.09 and WOG) to Drs VandenDriessche and Chuah; a research grant from the Research Foundation Flanders (G.0740.09.N10) to Dr Van de Werf; grants to Dr Sage from the Gilbertson Foundation and National Institute of Health (GM40711) and Ingenious Hypercare NoE from the European Union (EST 2005–020706–2); and research grants from the Netherlands Heart Foundation (2007B036, 2008B011) and a VIDI grant from the Netherlands Organization for Scientific Research to Dr Heymans. Dr Pinto is an established investigator of the Netherlands Heart Foundation.

Disclosures

None.

References

1. Susic D, Frohlich ED. The aging hypertensive heart: a brief update. *Nat Clin Pract*. 2008;5:104–110.
2. Spinale FG. Myocardial matrix remodeling and the matrix metalloproteinases: influence on cardiac form and function. *Physiol Rev*. 2007;87:1285–1342.
3. Schellings MW, Pinto YM, Heymans S. Matricellular proteins in the heart: possible role during stress and remodeling. *Cardiovasc Res*. 2004;64:24–31.
4. Bornstein P, Sage EH. Matricellular proteins: extracellular modulators of cell function. *Curr Opin Cell Biol*. 2002;14:608–616.
5. Schroen B, Heymans S, Sharma U, Blankesteijn WM, Pokharel S, Cleutjens JP, Porter JG, Evelo CT, Duisters R, van Leeuwen RE, Janssen BJ, Debets JJ, Smits JF, Daemen MJ, Crijns HJ, Bornstein P, Pinto YM. Thrombospondin-2 is essential for myocardial matrix integrity: increased expression identifies failure-prone cardiac hypertrophy. *Circ Res*. 2004;95:515–522.
6. Kyriakides TR, Leach KJ, Hoffman AS, Ratner BD, Bornstein P. Mice that lack the angiogenesis inhibitor, thrombospondin 2, mount an altered foreign body reaction characterized by increased vascularity. *Proc Natl Acad Sci U S A*. 1999;96:4449–4454.
7. Monreal G, Nicholson LM, Han B, Joshi MS, Phillips AB, Wold LE, Bauer JA, Gerhardt MA. Cytoskeletal remodeling of desmin is a more accurate measure of cardiac dysfunction than fibrosis or myocyte hypertrophy. *Life Sci*. 2008;83:786–794.
8. Krishnamurthy J, Torrice C, Ramsey MR, Kovalev GI, Al-Regaiey K, Su L, Sharpless NE. Ink4a/Arf expression is a biomarker of aging. *J Clin Invest*. 2004;114:1299–1307.
9. Lamy L, Foussat A, Brown EJ, Bornstein P, Ticchioni M, Bernard A. Interactions between CD47 and thrombospondin reduce inflammation. *J Immunol*. 2007;178:5930–5939.
10. Dai DF, Santana LF, Vermulst M, Tomazela DM, Emond MJ, MacCoss MJ, Gollahon K, Martin GM, Loeb LA, Ladiges WC, Rabinovitch PS. Overexpression of catalase targeted to mitochondria attenuates murine cardiac aging. *Circulation*. 2009;119:2789–2797.
11. Agah A, Kyriakides TR, Bornstein P. Proteolysis of cell-surface tissue transglutaminase by matrix metalloproteinase-2 contributes to the adhesive defect and matrix abnormalities in thrombospondin-2-null fibroblasts and mice. *Am J Pathol*. 2005;167:81–88.
12. Vanhoutte D, Schellings MW, Gotte M, Swinnen M, Herias V, Wild MK, Vestweber D, Chorianopoulos E, Cortes V, Rigotti A, Stepp MA, Van de Werf F, Carmeliet P, Pinto YM, Heymans S. Increased expression of syndecan-1 protects against cardiac dilatation and dysfunction after myocardial infarction. *Circulation*. 2007;115:475–482.
13. DeBosch B, Treskov I, Lupu TS, Weinheimer C, Kovacs A, Courtois M, Muslin AJ. Akt1 is required for physiological cardiac growth. *Circulation*. 2006;113:2097–2104.
14. Hannigan GE, Coles JG, Dedhar S. Integrin-linked kinase at the heart of cardiac contractility, repair, and disease. *Circ Res*. 2007;100:1408–1414.
15. Calzada MJ, Annis DS, Zeng B, Marcinkiewicz C, Banas B, Lawler J, Mosher DF, Roberts DD. Identification of novel beta1 integrin binding sites in the type 1 and type 2 repeats of thrombospondin-1. *J Biol Chem*. 2004;279:41734–41743.
16. Manning BD, Cantley LC. AKT/PKB signaling: navigating downstream. *Cell*. 2007;129:1261–1274.
17. Li M, Chiou KR, Bugayenko A, Irani K, Kass DA. Reduced wall compliance suppresses Akt-dependent apoptosis protection stimulated by pulse perfusion. *Circ Res*. 2005;97:587–595.
18. Donnini S, Morbidelli L, Taraboletti G, Ziche M. ERK1–2 and p38 MAPK regulate MMP/TIMP balance and function in response to thrombospondin-1 fragments in the microvascular endothelium. *Life Sci*. 2004;74:2975–2985.
19. Orr AW, Pallero MA, Xiong WC, Murphy-Ullrich JE. Thrombospondin induces RhoA inactivation through FAK-dependent signaling to stimulate focal adhesion disassembly. *J Biol Chem*. 2004;279:48983–48992.
20. Fischer P, Hilfiker-Kleiner D. Survival pathways in hypertrophy and heart failure: the gp130-STAT axis. *Basic Res Cardiol*. 2007;102:393–411.
21. DeBosch B, Sambandam N, Weinheimer C, Courtois M, Muslin AJ. Akt2 regulates cardiac metabolism and cardiomyocyte survival. *J Biol Chem*. 2006;281:32841–32851.
22. Kuhn B, del Monte F, Hajjar RJ, Chang YS, Lebeche D, Arab S, Keating MT. Periostin induces proliferation of differentiated cardiomyocytes and promotes cardiac repair. *Nat Med*. 2007;13:962–969.
23. Yoshida Y, Togi K, Matsumae H, Nakashima Y, Kojima Y, Yamamoto H, Ono K, Nakamura T, Kita T, Tanaka M. CCN1 protects cardiac myocytes from oxidative stress via beta1 integrin-Akt pathway. *Biochem Biophys Res Commun*. 2007;355:611–618.
24. Yang Z, Strickland DK, Bornstein P. Extracellular matrix metalloproteinase 2 levels are regulated by the low density lipoprotein-related scavenger receptor and thrombospondin 2. *J Biol Chem*. 2001;276:8403–8408.
25. Hayashidani S, Tsutsui H, Ikeuchi M, Shiomi T, Matsusaka H, Kubota T, Imanaka-Yoshida K, Itoh T, Takeshita A. Targeted deletion of MMP-2 attenuates early LV rupture and late remodeling after experimental myocardial infarction. *Am J Physiol Heart Circ Physiol*. 2003;285:H1229–H1235.
26. Agah A, Kyriakides TR, Letrondo N, Bjorkblom B, Bornstein P. Thrombospondin 2 levels are increased in aged mice: consequences for cutaneous wound healing and angiogenesis. *Matrix Biol*. 2004;22:539–547.
27. Bornstein P, Agah A, Kyriakides TR. The role of thrombospondins 1 and 2 in the regulation of cell-matrix interactions, collagen fibril formation, and the response to injury. *Int J Biochem Cell Biol*. 2004;36:1115–1125.
28. Du XJ. Gender modulates cardiac phenotype development in genetically modified mice. *Cardiovasc Res*. 2004;63:510–519.
29. Schellings MW, Vanhoutte D, Swinnen M, Cleutjens JP, Debets J, van Leeuwen RE, d'Hooge J, Van de Werf F, Carmeliet P, Pinto YM, Sage

EH, Heymans S. Absence of SPARC results in increased cardiac rupture and dysfunction after acute myocardial infarction. *J Exp Med*. 2009;206:113–123.
30. Heymans S, Luttun A, Nuyens D, Theilmeier G, Creemers E, Moons L, Dyspersin GD, Cleutjens JP, Shipley M, Angellilo A, Levi M, Nube O, Baker A, Keshet E, Lupu F, Herbert JM, Smits JF, Shapiro SD, Baes M, Borgers M, Collen D, Daemen MJ, Carmeliet P. Inhibition of plasminogen activators or matrix metalloproteinases prevents cardiac rupture but impairs therapeutic angiogenesis and causes cardiac failure. *Nat Med*. 1999;5:1135–1142.
31. Daya S, Berns KI. Gene therapy using adeno-associated virus vectors. *Clin Microbiol Rev*. 2008;21:583–593.

CLINICAL PERSPECTIVE

The incidence of heart failure increases with advanced aging. Still, some people get old (>80 years of age) without having their heart affected. With a healthy lifestyle and in the absence of hypertension, diabetes mellitus, or smoking, the heart is perfectly able to "endure" for a human lifetime. Identification of the protective mechanisms that allow the heart to age "for a long time" could lead to new therapeutic targets to delay its senescence and to treat heart failure in general. The present study proposes thrombospondin-2 as such a protective mechanism. The absence of this matrix protein in mice resulted in progressive dilated cardiomyopathy beginning in their middle age as a result of progressive cardiomyocyte death and matrix disruption. Importantly, overexpression of thrombospondin-2 via adeno-associated virus-9 gene transfer, a promising technique for gene therapy in human diseases, completely prevented this age-related cardiomyopathy. Thus, the postnatal presence of thrombospondin-2 is essential for "healthy" aging of the heart. Recent findings that modification of the extracellular environment by aging cells protects against age-related pathology should encourage the use of thrombospondin-2 and other matrix components as a novel therapeutic strategy for the prevention of heart failure in the aging individual.

Supplemental Material and methods

Expanded methods

AAV9-TSP-2 construction and production

AAV-CMV-GFP vectors expressed green fluorescent protein (GFP) from the human cytomegalovirus (CMV) promoter and were derived by cloning GFP into pAAV-MCS (Stratagene). AAV-CMV-TSP-2 vectors expressed TSP-2 from the CMV promoter and were derived by cloning TSP-2 into pAAV-MCS (Stratagene). Both vectors contained a b-globin intron downstream of CMV and a human growth hormone polyadenylation signal. 293 cells were cultured in Dulbecco's modified Eagle's medium (DMEM) supplemented with 2 mM L-glutamine (Gln), 100 IU/ml penicillin, 100 μg/ml streptomycin and 10% heat-inactivated fetal bovine serum (FBS, Invitrogen, Merelbeke, Belgium). AAV9-CMV-GFP or AAV9-CMV-TSP-2 vectors were produced at high-titer by calcium phosphate transfection of 293 cells with AAV-CMV-GFP or AAV-CMV-TSP-2 vector DNA, an adenoviral helper plasmid and AAV helper plasmids expressing AAV Rep_2 and AAV Cap_9 for production of AAV9 serotypes, as previously described.[1] Two days post-transfection, cells were lysed by successive freeze-thaw cycles and sonication. Lysates were treated with benzonase (Merck) and deoxycholate (Sigma-Aldrich) and subsequently subjected to three successive rounds of cesium chloride density ultracentrifugation. The fractions containing the AAV particles were

concentrated using an Amicon filter (Millipore) and washed with PBS 1mM $MgCl_2$. Vector titer was determined in triplicate and repeated twice by quantitative PCR analysis conducted on a ABI 7700 (Applied Biosystems) using Lux primers (Invitrogen) specific for the polyadenylation signal (primer sequences: Forward: *TCTATTGGGAACCAAGCTGGAGG* Reverse: *AGGAGGCGGAGATTGCAGTG*), as described previously. The standard consisted of serially diluted AAV-CMV-GFP vector plasmids of known quantity.

Immunohistochemical and electron microscopic analysis

After the study period, all mice were anaesthetized, and hearts were taken out and prepared for further histological and molecular analysis. Lungs, left (LV) and right ventricles (RV) were dissected, blotted dry and weighed. Immunostainings on paraffin sections were performed using antibodies against p16 (BD bioscience pharmingen, San Diego, CA), Laminin (Sigma), desmin (Abcam, Cambridge, MA), CD45 (BD Bioscience Pharmingen), active cleaved caspase-3 (Upstate Biotechnology, Euromedex, Souffelweyersheim, France), ubiquitin (Chemicon, Temecula, CA), α-smooth muscle cell actin (Dako, Leuven, Belgium), CD31 (Dako, Leuven, Belgium) and ε-lysyl γ-glutaminyl cross-links (Abcam, Cambridge, MA) as previously described.[2-4] For TSP-2 (BD Bioscience Pharmingen) sections were subsequently incubated with Biotin labeled secondary antibody followed by amplification with the signal amplification system steptavidin-HRP-C_fluorescein (Perkin Elmer). Nuclei were stained with DAPI (invitrogen).[3] The quantity of collagen

was determined as the percentage of Sirius Red staining area per total cardiac area.[2-5] The quality of the deposited collagen matrix was studied with Sirius Red polarization microscopy as previously described.[3, 4]

Morphometric analysis was performed with a Leitz DMRXE microscope (Leica Imaging systems Ltd), a 3CCD color video camera (CXC-93-OP, Sony) and a Leica Qwin software system by persons unaware of the genotype.

For electron microscopic scanning, hearts were treated with 1.5 % glutaraldehyde fixative buffered in 0.067 M cacodylate at pH 7.4. These hearts were washed in cacodylate buffer and transferred to a 1 % OsO4 fixative solution buffered with phosphate-buffered saline 0.1 M pH 7.4 for subsequent immersion fixation for 1 hour at 4°C. After washing in phosphate buffered saline 0.1 M pH 7.4, dehydration was carried out rapidly in graded ethanol series, followed by embedding in Epon. Hearts were examined at the University of Maastricht (EM unit, Molecular Cell biology) with a Philips CM 100 electron microscope (F.E.I., Eindhoven, The Netherlands) at an accelerating voltage of 80KV.

Zymographic MMP- and tissue transglutaminase activity with aging

Heart tissues were homogenized and extracted, and protein concentrations were determined. MMP-2 and MMP-9 zymographic activites were determined as described.[2] The activity of tissue transglutaminase (tTG), a collagen cross-linking enzyme which is inactivated by MMP-2, was measured in

homogenized heart tissues by incorporation of biotinylated cadaverine (BTC) into fibronectin as described.[4, 6]

RNA isolation and real time polymerase chain reaction

RNA was extracted from cardiac tissues using an RNeasy® Fibrous Tissue Mini Kit (Qiagen GmbH, Hilden, Germany) and was stored at -80°C. Transcript levels of *TSP-1, TSP-2, TSP-3, TSP-4*, *Superoxide Dismutase-2* (SOD2), *Glutathione peroxidase-1* (GPx1) and *Catalase1* (CAT1) were determined with a real-time fluorescence detection method as previously described[7] (Applied Biosystems), mouse *glyceraldehyde 3-phosphate dehydrogenase* (GAPDH) was used as an endogenous housekeeping gene. The primers used for this study are presented in supplemental table1.

Transcript levels of TGFβ, IL-1β, IL-6 and IL-12 were determined using TaqMan® low density arrays and were performed according to the manufacturer's instructions.[8] Each TaqMan® gene expression assay contains a forward and reverse primer for each of the chosen genes. 18S RNA was incorporated in our customized TaqMan Low-Density Array as internal standard.

Immunoblotting

Immunoblotting was performed on heart lysates for TSP-1 (kindly provided by Prof. Dr. M. Hoylaerts), TSP-2 (BD), TSP-3 (Santa Cruz biotechnology, Heidelberg, Germany) Integrin Linked kinase (ILK) (Cell signaling Technology

Inc., Beverly, MA, USA), Src (Cell singaling), protein kinase A or Akt (Cel signaling) and their phosphorylated forms, and GAPDH (cell signaling) as previously described.[3, 4] Protein levels were expressed relative to protein levels of GAPDH.

ILK activity and active TGF beta assays

Immunoprecipitation of ILK in TSP-2 KO and WT heart homogenates together with the kinase activity assay were carried out as detailed in Weaver M. et al.[9]

To determine active TGF-β1 protein levels, a TGF-β1 assay was performed according to the manufacturer's instructions (R&D systems, Minneapolis, MN, USA). Cardiac tissue extracts were pre-adjusted to 1.0 mg/mL in protein.[10]

Echocardiographic measurements

Transthoracic echocardiographic examination was performed using a 13-mHz transducer (i13L, GE Vingmed, Horten, Norway) on a Vingmed Vivid 7 scanner (GE Vingmed,Horten, Norway) in anesthetized mice (2% isoflurane). LV diameters at end-diastole (LVEDD) and end-systole (LVESD), septal wall thickness (SW diast), and LV posterior wall in end diastole (PW diast) were measured, and fractional shortening (FS) was calculated as described previously.[5, 11]

In vitro experimental approaches

A rat TSP-2 (rTSP-2) short hairpin RNA (shRNA)-expressing lentiviral vector was generated by annealing complementary shTSP-2 oligonucleotides (Supplemental table 1) and ligating them into HpAI-XhoI-digested pLL3.7 puro vector DNA (modified from a donation by L. van Parijs, Massachusetts Institute of Technology, Cambridge, MA). Lentiviral production was performed as described previously, and viral supernatant was harvested after 48 hours.[12] Neonatal rat ventricular cardiac myocytes (NRCMs) were isolated by enzymatic disassociation of 1- to 2-days-old neonatal rat hearts.

As neonatal hearts produce a significant amount of TSP-2 –at least- until 6 days after birth[13], the use of NRCMs was suitable for our experimental setup. NRCMs were infected with lentivirus containing shRNA against TSP-2 or unrelated shRNA lentiviral vector (control; Sigma) and harvested after 10 days as previously described.[12]

Mouse monoclonal anti-TSP antibodies, Ab.3 clone C6.7 (indicated as α-TSP^{CD47}) and Ab.1 clone A4.1 (indicated as α-TSP^{CD36}) (Labvision Corporation, Duiven, the Netherlands), were used to block respectively the CD47 binding site (C terminal domain) and the CD36 binding site respectively on TSP-1 and TSP-2.[14] Cell lysates were prepared for further analysis of protein expression and transcript levels.

Force measurements in single permeabilized cardiomyocytes

Force measurements were performed in single, mechanically isolated cardiomyocytes as described previously. [15, 16] Cardiac samples were defrosted

in relaxing solution (free Mg 1, KCl 100, EGTA 2, Mg-ATP 4 and imidazole 10 mmol/L; pH 7.0), mechanically disrupted and incubated for 5 minutes in relaxing solution supplemented with 0.5% Triton X-100 to remove all membrane structures. Subsequently, cells were washed twice in relaxing solution, after which single cardiomyocytes were attached with silicone adhesive between a force transducer and a motor. Sarcomere length of isolated cardiomyocytes was adjusted to 2.2 μm and myocytes were subjected to both relaxing and activating solutions. Their pCa ($-_{10}\log[Ca^{2+}]$) ranged from 9.0 (relaxing) to 4.5 (maximal activation), which was used to calculate maximal calcium-activated isometric force. All force values were normalized for cardiomyocyte cross-sectional area. Exposure to a series of solutions with intermediate pCa yielded the baseline force-pCa relation. On transfer of the myocyte from relaxing to activating solution, isometric force started to develop. Once a steady force level was reached, the cell was shortened within 1 ms to 80% of its original length (slack test) to determine the baseline of the force transducer. The distance between the baseline and the steady force level is the total force (Ftotal). After 20 ms, the cell was restretched and returned to the relaxing solution, in which a second slack test of 10-seconds' duration was performed to determine passive $F_{passive}$. The difference between Ftotal and Fpassive equalled Factive. Ca^{2+}-sensitivity of the contractile apparatus (pCa_{50}) corresponded to the pCa, at which Factive reached 50% of the value observed at maximal activation. After measurement of the baseline force-pCa relation, myocytes were incubated for 40 minutes in relaxing solution supplemented with the catalytic subunit of

protein kinase A (PKA, 100 U/mL; Sigma, batch-12K7495) and 6 mmol/L dithiothreitol (DTT, MP-Biochemicals).

Phosphorylation status of myofilament proteins

Myofilament protein phosphorylation was determined using Pro-Q Diamond Phosphoprotein Stain as described previously.[17] To preserve the endogenous phosphorylation status, frozen samples were homogenized in liquid nitrogen and re-suspended in 1 mL cold 10% trichloroacetic acid solution (TCA; dissolved in acetone containing 0.1% (w/v) DTT. TCA-treated tissue pellets were homogenized in sample buffer containing 15% glycerol, 62.5 mM Tris (pH 6.8), 1% (w/v) SDS and 2% (w/v) DTT. Tissue samples were separated on gradient gels (Criterion tris-HCl 4-15% gel, BioRad) and proteins were stained for one hour with Pro-Q Diamond Phosphoprotein Stain. Fixation, washing and de-staining were performed according to the manufacturer's guidelines (Molecular Probes). To assess protein content subsequently gels were stained overnight with SYPRO Ruby stain (Molecular Probes). Phosphorylation status of myofilament proteins was expressed relative to protein expression of cardiac myosin-binding protein C (MyBP-C) to correct for differences in sample loading. Staining was visualized using the LAS-3000 Image Reader and signals were analyzed with AIDA.

Supplemental References

1. Vandendriessche T, Thorrez L, Acosta-Sanchez A, Petrus I, Wang L, Ma L, L DEW, Iwasaki Y, Gillijns V, Wilson JM, Collen D, Chuah MK. Efficacy and safety of adeno-associated viral vectors based on serotype 8 and 9 vs. lentiviral vectors for hemophilia B gene therapy. *J Thromb Haemost.* 2007;5(1):16-24.

2. Heymans S, Luttun A, Nuyens D, Theilmeier G, Creemers E, Moons L, Dyspersin GD, Cleutjens JP, Shipley M, Angellilo A, Levi M, Nube O, Baker A, Keshet E, Lupu F, Herbert JM, Smits JF, Shapiro SD, Baes M, Borgers M, Collen D, Daemen MJ, Carmeliet P. Inhibition of plasminogen activators or matrix metalloproteinases prevents cardiac rupture but impairs therapeutic angiogenesis and causes cardiac failure. *Nat Med.* Vol 5; 1999:1135-1142.

3. Schellings MW, Vanhoutte D, Swinnen M, Cleutjens JP, Debets J, van Leeuwen RE, d'Hooge J, Van de Werf F, Carmeliet P, Pinto YM, Sage EH, Heymans S. Absence of SPARC results in increased cardiac rupture and dysfunction after acute myocardial infarction. *J Exp Med.* 2009;206(1):113-123.

4. Vanhoutte D, Schellings MW, Gotte M, Swinnen M, Herias V, Wild MK, Vestweber D, Chorianopoulos E, Cortes V, Rigotti A, Stepp MA, Van de Werf F, Carmeliet P, Pinto YM, Heymans S. Increased expression

of syndecan-1 protects against cardiac dilatation and dysfunction after myocardial infarction. *Circulation.* 2007;115(4):475-482.

5. Heymans S, Lupu F, Terclavers S, Vanwetswinkel B, Herbert JM, Baker A, Collen D, Carmeliet P, Moons L. Loss or Inhibition of uPA or MMP-9 Attenuates LV Remodeling and Dysfunction after Acute Pressure Overload in Mice. *Am J Pathol.* 2005;166(1):15-25.

6. Agah A, Kyriakides TR, Bornstein P. Proteolysis of cell-surface tissue transglutaminase by matrix metalloproteinase-2 contributes to the adhesive defect and matrix abnormalities in thrombospondin-2-null fibroblasts and mice. *Am J Pathol.* 2005;167(1):81-88.

7. Dai DF, Santana LF, Vermulst M, Tomazela DM, Emond MJ, MacCoss MJ, Gollahon K, Martin GM, Loeb LA, Ladiges WC, Rabinovitch PS. Overexpression of catalase targeted to mitochondria attenuates murine cardiac aging. *Circulation.* 2009;119(21):2789-2797.

8. Abruzzo LV, Lee KY, Fuller A, Silverman A, Keating MJ, Medeiros LJ, Coombes KR. Validation of oligonucleotide microarray data using microfluidic low-density arrays: a new statistical method to normalize real-time RT-PCR data. *BioTechniques.* 2005;38(5):785-792.

9. Weaver MS, Workman G, Sage EH. The copper binding domain of SPARC mediates cell survival in vitro via interaction with integrin beta1 and activation of integrin-linked kinase. *J Biol Chem.* 2008;283(33):22826-22837.

10. Mo W, Brecklin C, Garber SL, Song RH, Pegoraro AA, Au J, Arruda JA, Dunea G, Singh AK. Changes in collagenases and TGF-beta precede

structural alterations in a model of chronic renal fibrosis. *Kidney international.* 1999;56(1):145-153.

11. Schroen B, Heymans S, Sharma U, Blankesteijn WM, Pokharel S, Cleutjens JP, Porter JG, Evelo CT, Duisters R, van Leeuwen RE, Janssen BJ, Debets JJ, Smits JF, Daemen MJ, Crijns HJ, Bornstein P, Pinto YM. Thrombospondin-2 is essential for myocardial matrix integrity: increased expression identifies failure-prone cardiac hypertrophy. *Circ Res.* 2004;95(5):515-522.

12. Schroen B, Leenders JJ, van Erk A, Bertrand AT, van Loon M, van Leeuwen RE, Kubben N, Duisters RF, Schellings MW, Janssen BJ, Debets JJ, Schwake M, Hoydal MA, Heymans S, Saftig P, Pinto YM. Lysosomal integral membrane protein 2 is a novel component of the cardiac intercalated disc and vital for load-induced cardiac myocyte hypertrophy. *J Exp Med.* 2007;204(5):1227-1235.

13. Iruela-Arispe ML, Liska DJ, Sage EH, Bornstein P. Differential expression of thrombospondin 1, 2, and 3 during murine development. *Dev Dyn.* 1993;197(1):40-56.

14. Calzada MJ, Annis DS, Zeng B, Marcinkiewicz C, Banas B, Lawler J, Mosher DF, Roberts DD. Identification of novel beta1 integrin binding sites in the type 1 and type 2 repeats of thrombospondin-1. *J Biol Chem.* 2004;279(40):41734-41743.

15. van der Velden J, Papp Z, Boontje NM, Zaremba R, de Jong JW, Janssen PM, Hasenfuss G, Stienen GJ. The effect of myosin light

chain 2 dephosphorylation on Ca2+ -sensitivity of force is enhanced in failing human hearts. *Cardiovasc Res.* 2003;57(2):505-514.

16. van der Velden J, Papp Z, Zaremba R, Boontje NM, de Jong JW, Owen VJ, Burton PB, Goldmann P, Jaquet K, Stienen GJ. Increased Ca2+-sensitivity of the contractile apparatus in end-stage human heart failure results from altered phosphorylation of contractile proteins. *Cardiovasc Res.* 2003;57(1):37-47.

17. Zaremba R, Merkus D, Hamdani N, Lamers J, Paulus W, C. dR, Duncker D, Stienen G, van der Velden J. Quantitative analysis of myofilament protein phosphorylation in small cardiac biopsies. *Proteomics Clinical Application.* 2007;1(10):1285-1290.

Supplemental figure legends

Supplemental Figure 1: The loss of TSP-2 resulted in increased cardiac fibrosis .

(A-E) Post mortem analysis of Sirius red–stained older male TSP-2 KO hearts revealing increased cardiac fibrosis and cardiomyocyte dropout. A-E represent 4 individual hearts.

Bars: (A-H) 100 μm

Supplemental Figure 2: The loss of TSP-2 did not resulted in differences in ILK activity levels with aging

(A) Immunoblotting for ILK protein levels did not show differences in young and older TSP-2 KO hearts as compared with age-matched WT littermates (n=5 per genotype per age-group; *P*=NS). (B). ILK activity assay showed no significant differences in ILK activity levels between TSP-2 KO and WT hearts in young or older mice.

Supplemental Table 1. List of primers for Real-Time PCR and for shTSP-2 production

Gene	Primer	Sequence 5'-3'
Mouse-	F	5'-ACGTGCCGCCTGGAGA-3'
GAPDH[a]	R	5'-CCCTCAGATGCCTGCTTCA-3'
	Probe	5'-CACCTTCTTGATGTCATCATACTTGGCAGG-3'
Mouse-	F	5'-CCTGGCATCGGAGCCCA-3'
CAT1	R	5'-GTGTCCGGGTAGGCAAAAAG-3'
`	Probe	5'-CCCTGACAAAATGCTTCAGGGCCG-3'
Mouse-	F	5'-GACTGGTGGTGCTCGGTTTC-3'
Gxp	R	5'-CAGAATCTCTTCATTCTTGCCAT-3'
	Probe	5'-CGTGCAATCAGTTCGGACACCAGG-3'
Rat-	Sense	5'-GATATCTGCTTCTCAATTA**TTCAAGAGA**TAATTGAGAAGCAGATATC**TTTTTC**–3'
shTSP-2[b]	Antisense	5'-TCGAGAAAAA**GATATCTGCTTCTCAATTA**TCTCTTGAA**TAATTGAGAAGCAGATATC**–3'

[a]Housekeeping gene: GAPDH,glyceraldehydes3-phhosphate dehydrogenase

[b]rat-shTSP-2 oligonucleotides, Hairpin structure in bold.

Mouse TSP-1 ID: Mm 01335419_g1; Mouse TSP-2 ID: Mm01279241_m1;

Mouse TSP-3 ID: Mm 01212335_m1; Mouse TSP-4 ID: Mm 03003598_s1

Mouse SOD2 ID: Mm 00449726_m1

Supplemental Figure 1

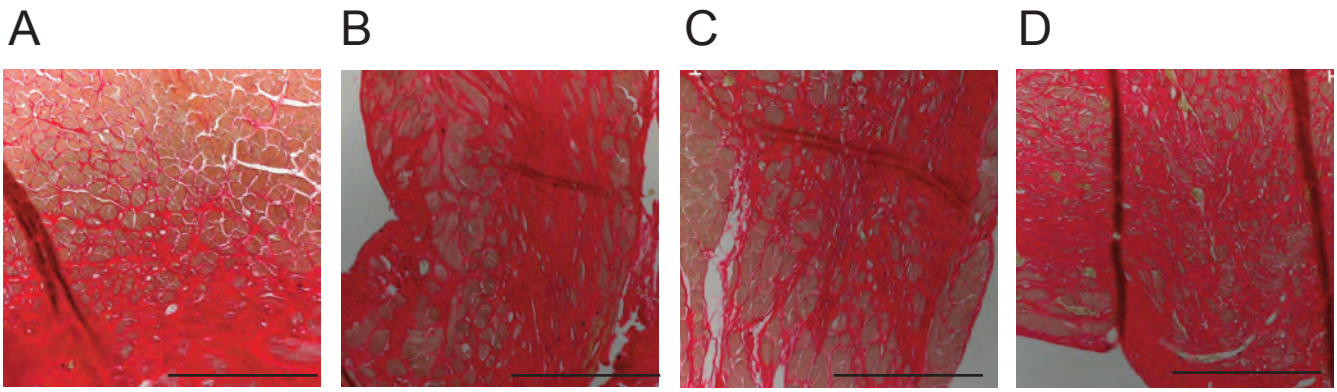

Supplemental figure 2